

## Aromaticity Reversal

Deutsche Ausgabe: DOI: 10.1002/ange.201603631  
Internationale Ausgabe: DOI: 10.1002/anie.201603631

## A Description of Vibrational Modes in Hexaphyrins: Understanding the Aromaticity Reversal in the Lowest Triplet State

Young Mo Sung, Juwon Oh, Koji Naoda, Taegon Lee, Woojae Kim, Manho Lim,\*  
Atsuhiko Osuka,\* and Dongho Kim\*

**Abstract:** Aromaticity reversal in the lowest triplet state, or Baird's rule, has been postulated for the past few decades. Despite numerous theoretical works on aromaticity reversal, experimental study is still at a rudimentary stage. Herein, we investigate the aromaticity reversal in the lowest excited triplet state using a comparable set of [26]- and [28]hexaphyrins by femtosecond time-resolved infrared (IR) spectroscopy. Compared to the relatively simple IR spectra of [26]bis(rhodium) hexaphyrin (**R26H**), those of [28]bis(rhodium) hexaphyrin (**R28H**) show complex IR spectra the region for the stretching modes of conjugated rings. Whereas time-resolved IR spectra of **R26H** in the excited triplet state are dominated by excited state IR absorption peaks, while those of **R28H** largely show ground state IR bleaching peaks, reflecting the aromaticity reversal in the lowest triplet state. These contrasting IR spectral features serve as new experimental aromaticity indices for Baird's rule.

Aromaticity has been regarded as one of the most important concepts in physical organic chemistry because the chemical stabilities and reactivities of molecules could be predicted by their degree of aromaticity and antiaromaticity.<sup>[1]</sup> According to Hückel's  $[4n+2]$  rule,<sup>[2]</sup> the aromaticity of planar annulenes could be predicted by counting the number of  $\pi$ -electrons;  $[4n+2]\pi$ -electronic systems show aromatic features, while annulenes having  $[4n]\pi$ -electrons exhibit antiaromatic ones. This electron counting rule to predict the aromaticity and antiaromaticity could be reversed in the lowest triplet state of annulenes, which is known as Baird's rule.<sup>[3]</sup> With increasing attention to Baird's pioneering work,

the concept of aromaticity reversal in the lowest triplet state of annulenes has been an interesting research topic as illustrated by a significant body of theoretical and experimental research because of its substantial potential applications in organic synthetic photochemistry.<sup>[4–17,21–23]</sup> At the early stage in the development of this interesting concept, only theoretical works based on various aromatic indices, such as aromatic stabilization energy, nucleus-independent chemical shifts, and harmonic oscillator model of aromaticity, were reported because the experimental aromaticity indices for the excited state have not yet been established. In the 2000s, with an analysis of fulvene having chameleon spectroscopic features reported by Ottosson et al.<sup>[5,17–21]</sup> quantitative experimental research for the aromaticity reversal has been conducted.<sup>[24–26]</sup> Recently, we have demonstrated the aromaticity reversal in the excited singlet and triplet states of a comparable set of [26]- and [28]hexaphyrins by investigating their absorption spectral differences between the ground and excited states along with quantum mechanical calculations, which provides the spectroscopic evidence of Baird's rule.<sup>[27,28]</sup> In previous work, we observed the changes in the electronic transitions of [26]- and [28]hexaphyrins in the excited states, hexaphyrins having aromatic character ([26]hexaphyrins in the ground state and [28]hexaphyrins in the triplet state) exhibit sharp and intense absorption spectra, while antiaromatic hexaphyrins ([26]hexaphyrins in the triplet state and [28]hexaphyrins in the ground state) show broad and weak absorption spectra.<sup>[27–29]</sup> Considering the relationship between the electronic structures and molecular structures, we could suggest that aromatic hexaphyrins exhibit different molecular structures from antiaromatic hexaphyrins in the process of aromaticity reversal in the excited triplet state. This feature comes forth with a new possibility to set experimental indices in relation to the molecular structures for the aromaticity reversal in the lowest excited triplet state.

Vibrational spectroscopy has been well established as one of the most effective methods to explore the molecular structures. IR spectroscopy, one of fundamental vibrational spectroscopies, is widely recognized as a useful tool to characterize the vibrational modes in the ground state.<sup>[30]</sup> With the advent of femtosecond laser pulses, femtosecond time-resolved IR spectroscopy has developed very rapidly, which enables us to observe the structural changes during photochemical processes taking place in a few hundred femtoseconds.<sup>[31,32]</sup> The enlightenment of ultrafast phenomena occurring in the excited state of molecular systems, such as photosynthetic process, would be expected to provide valuable clues to control and modify the molecular dynamics in the excited state. In this regard, herein, the vibrational

[\*] Dr. Y. M. Sung, J. Oh, W. Kim, Prof. Dr. D. Kim  
Spectroscopy Laboratory for Functional  $\pi$ -electronic systems and  
Department of Chemistry  
Yonsei University  
Seoul 120-749 (Korea)  
E-mail: dongho@yonsei.ac.kr  
K. Naoda, Prof. Dr. A. Osuka  
Department of Chemistry, Graduate School of Science  
Kyoto University  
Sakyo-ku, Kyoto 606-8502 (Japan)  
E-mail: osuka@kuchem.kyoto-u.ac.jp  
Dr. T. Lee, Prof. Dr. M. Lim  
Department of Chemistry and Chemistry Institute for Functional  
Materials  
Pusan National University  
Busan 609-735 (Korea)  
E-mail: mhlhm@pusan.ac.kr

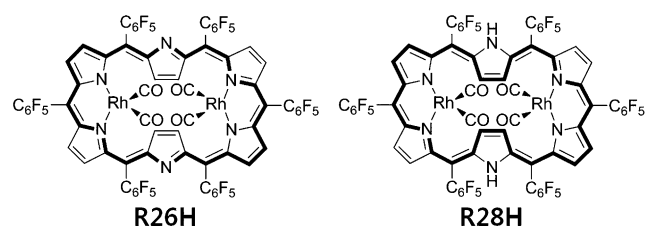
Supporting information for this article can be found under:  
<http://dx.doi.org/10.1002/anie.201603631>.

modes in the triplet state of a comparable set of aromatic and antiaromatic expanded porphyrins having the same molecular framework but different number of  $\pi$ -electrons have been investigated by femtosecond time-resolved IR spectroscopy to probe the structural changes in relation to the aromaticity reversal in the triplet excited state as recognized by Baird's rule.

As has been established, IR spectroscopy provides information on the vibrational modes of the molecule, showing allowed transitions in the case of periodic change of dipole moments. In general, in the stretching vibrational modes of planar annulene molecules, IR-active vibrational modes would be antisymmetric stretching ones inducing a change in the dipole moment, while IR-forbidden vibrational modes would be symmetric stretching ones which can cause no net-change in the dipole moment. Furthermore, femtosecond time-resolved IR spectroscopy could allow us to observe IR spectral changes taking place in ultrafast time scale, which facilitates predicting the change of molecular structures. Considering that a switching from aromaticity (antiaromaticity) to antiaromaticity (aromaticity) in the lowest triplet state would cause the structural distortions due to the energetic instability of antiaromatic molecules, it could be expected that femtosecond time-resolved IR spectroscopy would provide a new experimental evidence on the aromaticity reversal in the excited triplet state.

Generally, it is difficult to synthesize stable aromatic and antiaromatic annulenic compounds exhibiting an obvious distinction in chemical and photophysical properties between the ground and lowest triplet states. However, expanded porphyrins, containing more than four pyrrole or pyrrole related rings, are ideally suited for a study of the aromaticity reversal in the excited state, because the distinctive photophysical and chemical properties depending on their aromaticity and antiaromaticity have been reported with photostability.<sup>[33–36]</sup> In this regard, to investigate the vibrational mode changes in conjunction with the aromaticity reversal in the lowest triplet states, we have prepared a comparable set of [26]- and [28]bis(rhodium) hexaphyrins, **R26H** (aromatic) and **R28H** (antiaromatic) having  $D_{2h}$  symmetry (Scheme 1),<sup>[29]</sup> which show chemically stable states, the fast intersystem crossing causing a prompt population of the triplet state and distinct absorption spectral changes in the lowest triplet state compared to the ground state.<sup>[27]</sup>

Herein, we attempted to reveal the structural changes of **R26H** and **R28H** by femtosecond time-resolved IR spectroscopy in conjunction with the aromaticity reversal in the excited triplet state. As a reference we measured the ground state IR spectra of **R26H** and **R28H** (Figure 1), which shows



Scheme 1. Chemical structures of **R26H** and **R28H**.

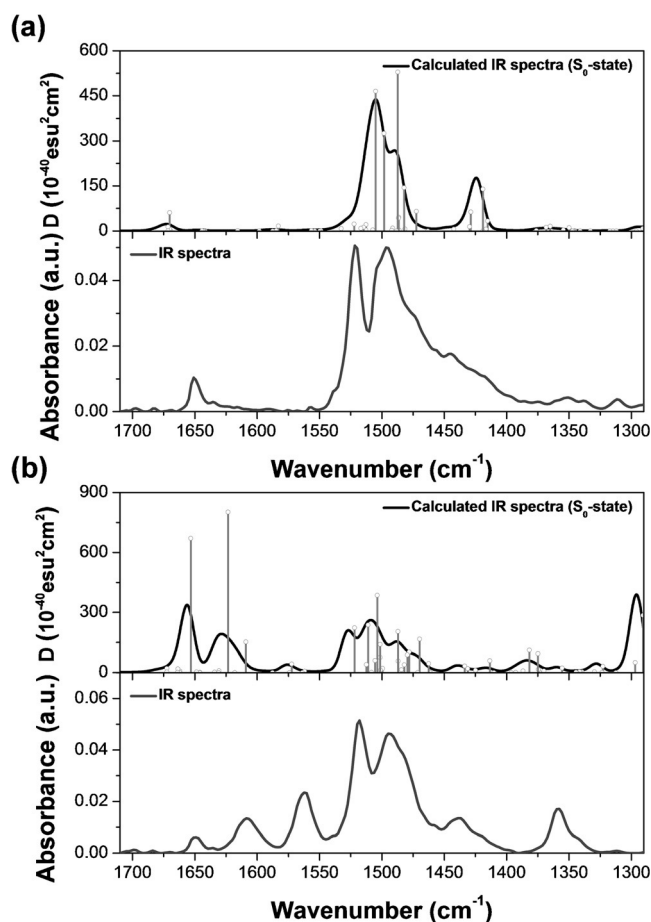
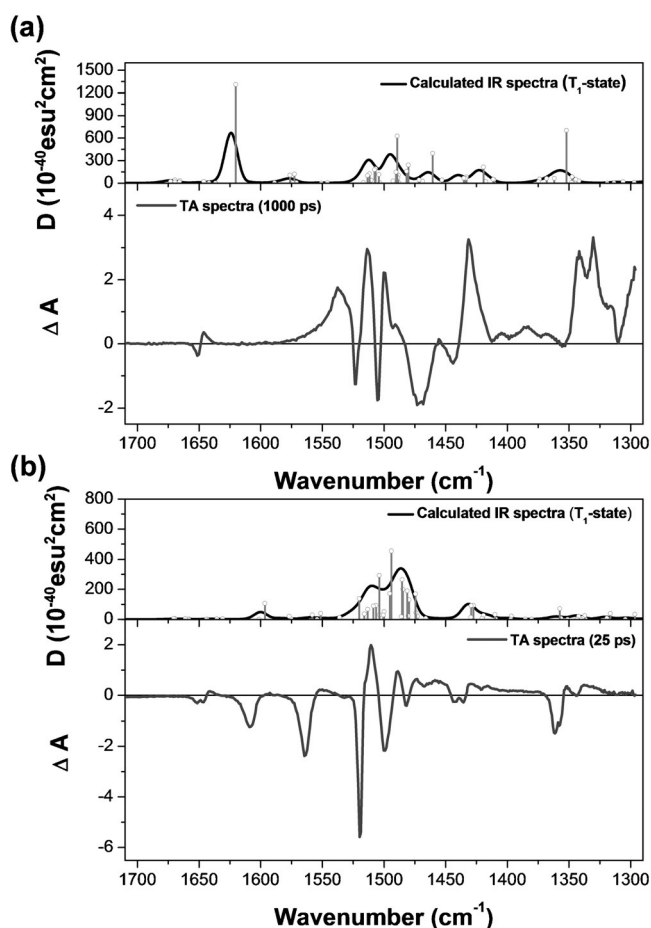


Figure 1. a) Calculated ground state IR-active spectrum (top) and IR spectrum (bottom) of **R26H**. b) Calculated ground state IR-active spectrum (top) and IR spectrum (bottom) of **R28H**.

quite different spectra from each other in 1300–1700  $\text{cm}^{-1}$  region where the stretching modes of conjugated ring can be detected. For **R26H**, we observed strong bands around 1500 and 1520  $\text{cm}^{-1}$  with a shoulder at 1450  $\text{cm}^{-1}$ . And a relatively weak band at 1650  $\text{cm}^{-1}$  was also observed. In contrast, for **R28H** in addition to those IR bands as observed in **R26H**, several additional bands appear at 1358, 1562 and 1608  $\text{cm}^{-1}$ , indicating that there is a difference in the ground state structure between **R26H** and **R28H**. To monitor the structural changes of **R26H** and **R28H** in the excited triplet state, we have carried out femtosecond time-resolved IR spectroscopic experiments (visible pump and IR probe) by controlling a time delay between pump and probe pulses to exclusively monitor the triplet excited state (Figure 2 and Figure S1 in the Supporting Information). We can notice that the ground state bleaching peaks in the transient IR spectra of **R26H** and **R28H** are well matched with the ground state IR spectra. In the time-resolved IR spectra, **R28H** displays the simple excited state IR bands around 1510  $\text{cm}^{-1}$ , while **R26H** exhibits additional excited state IR bands around 1340, 1540, and 1650  $\text{cm}^{-1}$  as well as the band around 1510  $\text{cm}^{-1}$  which was observed in **R28H**. Comparing the IR spectra in the ground state with the time-resolved IR spectra of **R26H** and **R28H**, we can see easily that **R26H** and **R28H** show reversed IR



**Figure 2.** a) Calculated lowest triplet state IR-active spectrum (top) and time-resolved IR spectrum (bottom) of **R26H**. b) Calculated lowest triplet state IR-active spectrum (top) and time-resolved IR spectrum (bottom) of **R28H**.

spectral features; the simple IR spectra of **R26H** in the ground state become complex in the lowest triplet state, while the complicated IR spectra of **R28H** in the ground state become relatively simpler in the lowest triplet state (Figures S2, S3).

To explore the origin for the reversed IR spectral features in the lowest triplet state of bis(rhodium) hexaphyrins, we have calculated the IR-active vibrational modes of **R26H** and **R28H** in the ground and lowest triplet states at the (U)B3LYP/LANL2DZP level (Figures 1 and Figure 2). First, the calculated ground state IR spectra of **R26H** are consistent with the observed IR spectra. On the other hand, although the calculated IR spectra of **R28H** are roughly matched with the observed IR spectra, there are large discrepancies especially in the intensity of each IR band.

For planar aromatic **R26H** molecule, the IR spectra are mainly contributed by symmetric in-plane vibrational modes, suggesting that the optimized structure represents well the actual geometry of **R26H**. In contrast, a rather distorted antiaromatic **R28H** molecule, the IR spectra has additional contributions by out-of-plane asymmetric vibrational motions which give rise to an appearance of new IR bands at 1360, 1510 and 1610  $\text{cm}^{-1}$ . Since the relative intensities of IR bands

are sensitive to the overall molecular structures, the optimized geometry of **R28H** does not seem to be fully consistent with the ground state structure of **R28H**. This feature is likely to be a reason for an inconsistency especially in the intensities of IR bands between the calculated IR spectra and observed ones of **R28H**. Nevertheless, the overall features in the IR spectra clearly represent the structural differences in the IR spectra of aromatic **R26H** and antiaromatic **R28H** molecules. Overall, **R26H** shows weak or forbidden vibrational modes in 1300–1400 and 1550–1650  $\text{cm}^{-1}$  frequency regions, while **R28H** exhibits allowed vibrational modes around 1370, 1510, and 1620  $\text{cm}^{-1}$ . These vibrational modes are the stretching modes in which all atoms in macrocyclic conjugated pathway are concerted; the vibrational modes around 1370, 1510, and 1620  $\text{cm}^{-1}$  are C–H bending modes with weak C–C stretching modes, C–C stretching modes with weak C–H bending modes, and C–C stretching modes, respectively. It is likely that these calculated IR-active bands reflect the aromaticity of bis(rhodium) hexaphyrins because these stretching modes are active along the conjugated pathway. As for the dipole strength of **R26H** and **R28H** exhibiting comparable vibrational modes in similar frequency region, the IR activities of **R26H** at 1376 ( $A_g$ ), 1515 ( $A_g$ ), and 1598 ( $A_g$ )  $\text{cm}^{-1}$  were recorded to be 2.56, 20.60, and 0.54, respectively, while those of **R28H** at 1382 ( $B_{3u}$ ), 1511 ( $B_{3u}$ ), and 1623 ( $B_{2u}$ )  $\text{cm}^{-1}$  were estimated to be 210.94, 448.10, and 1514.86, respectively (Figures S4 and S5, Table S1). Accordingly, these three distinctively allowed bands at 1382, 1511, and 1623  $\text{cm}^{-1}$  in the calculated vibrational spectra of **R28H** correspond to 1358, 1562, and 1608  $\text{cm}^{-1}$  bands in the observed IR spectra, respectively.

To illustrate the calculated and experimental IR spectra in the lowest triplet state, the transient IR species were selectively chosen at different time delays, 1000 ps for **R26H** and 25 ps for **R28H** (Figure 2) by considering the intersystem crossing rates and triplet state lifetimes of **R26H** (17 and > 5000 ps) and **R28H** (11 and 195 ps),<sup>[27]</sup> which reflect the triplet state IR spectra. These selected transient IR spectra are in good accordance with the calculated triplet state IR spectra (Figure 2). Furthermore, on the contrary to the ground state IR spectra of bis(rhodium) hexaphyrins, their calculated and experimental triplet state vibrational spectra are interconvertible with those of counterpart congener in the ground state; the calculated IR-active vibrational features of **R26H** in the lowest triplet state are similar to those of **R28H** in the ground state, while the estimated IR-active vibrational modes of **R28H** in the lowest triplet state are analogous to those of **R26H** in the ground state (Figure 2). The calculated triplet IR-active vibrational modes of **R28H** in 1300–1400 and 1550–1620  $\text{cm}^{-1}$  region are silent, while the calculated triplet IR spectra of **R26H** exhibit allowed vibrational modes around 1370, 1510, and 1610  $\text{cm}^{-1}$ . The IR-activities of **R28H** at 1380 ( $B_{1g}$ ), 1516 ( $B_{3g}$ ), and 1601 ( $B_{1g}$ )  $\text{cm}^{-1}$  were estimated to be 3.11, 45.75, and 0.10, respectively, while those of **R26H** at 1371 ( $B_{3u}$ ), 1512 ( $B_{3u}$ ), and 1611 ( $B_{2u}$ )  $\text{cm}^{-1}$  to be 58.37, 202.03, and 1489.99, respectively (Figures S6 and S7, Table S1). These unique calculated vibrational modes of **R26H** in the lowest triplet state at 1342, 1512, and 1611  $\text{cm}^{-1}$  could be assigned as the excited state IR bands in the time-resolved IR spectra



around 1340, 1530, and 1640  $\text{cm}^{-1}$ . As a consequence, the calculated vibrational modes of **R26H** in the triplet state are similar to those of the ground state of **R28H**. This complete reversal in the vibrational modes was also observed in the case of **R28H** (Table S1). These completely reversed features of vibrational modes in the lowest triplet state illustrate that the relatively planar (distorted) aromatic (antiaromatic) hexaphyrins become distorted (planar), leading to an enhancement (suppression) of out-of-plane vibrational modes in the excited triplet state, reinforcing the reversal of aromaticity in the triplet state, Baird's rule. Although the out-of-plane modes of porphyrinoids largely occur below 1000  $\text{cm}^{-1}$ ,<sup>[37]</sup> the out-of-plane vibrational modes of bis(rhodium) hexaphyrins combined with the C–C stretching modes, which enables them to occur in higher wavenumber region. Accordingly, the IR spectra of **R26H** and **R28H** exhibit contrasting features between the ground and excited triplet states, which demonstrates the reversal of aromaticity in view of structural changes in the excited triplet state.

To understand the effect of distorted and asymmetric structures of hexaphyrins on their three distinctive vibrational modes, we have analyzed the mean-plane deviation which represents the degree of structural distortions (Figure 3).<sup>[38,39]</sup> The mean plane deviation of **R26H** (0.266 Å) in the ground state shows smaller values compared to that of **R28H** (0.381 Å). In contrast with the ground state calculations, the mean-plane deviation value of **R26H** (0.321 Å) in the lowest triplet state was evaluated to be larger than that of **R28H** (0.276 Å). These results indicate that the more distorted structures of antiaromatic hexaphyrins cause the forbidden vibrational modes in planar structures to be allowed. Thus, some peculiar bands of antiaromatic hexaphyrins are induced by their distorted structures, whereas those of aromatic

hexaphyrins are still forbidden because of its relatively planar structures. In other words, the forbidden vibrational modes in the IR spectra of aromatic expanded porphyrins become allowed in antiaromatic expanded porphyrins having the same molecular framework but different number of  $\pi$ -electrons.

To clearly address this issue, we have calculated the vibrational modes by changing the dihedral angles of pyrrole rings in the optimized structures of **R26H** from 0 to 30 degree (Figures S8 and S9). As the topology of **R26H** changes, the IR activities of these vibrational modes are enhanced around 1350, 1520, and 1660  $\text{cm}^{-1}$ . The vibrational modes of these three IR bands are well matched with the unique allowed vibrational modes for antiaromatic hexaphyrins (**R26H** in the lowest triplet state and **R28H** in the ground state). This result indicates that the distorted and asymmetric geometry of hexaphyrins could bring out the allowed vibrational modes in the IR spectra. Considering that the antiaromaticity of hexaphyrins gives rise to the distortion of molecular structures due to the energetic instability, it could be assumed that this clear discrepancy between the vibrational modes of planar and distorted hexaphyrins reflects a switching between aromaticity and antiaromaticity. Moreover, the reversed features of vibrational modes in the lowest triplet state of hexaphyrins compared to the ground state suggest that the distorted (planar) structures of antiaromatic (aromatic) expanded porphyrins in the ground state become relatively planar (distorted) in the lowest triplet state, which is in good agreement with our previous works on the reversal of aromaticity of hexaphyrins.<sup>[27,28]</sup>

In conclusion, the IR spectra of aromatic and antiaromatic bis(rhodium) hexaphyrins provide a distinguishable mark for discriminating the aromatic and antiaromatic hexaphyrins. In addition, the aromaticity reversal in the lowest triplet state of hexaphyrins could be deduced from the combination of experimental results and quantum mechanical calculations. To the our knowledge, this is the first demonstration using vibrational spectroscopy to reveal the (anti)aromaticity reversal. Moreover, it is expected that this result will provide us with useful information on regulating the molecular structures in the excited states, and as a consequence, it will lead us to understand the underlying mechanisms on the aromaticity reversal.

## Acknowledgements

This work at Yonsei University was supported by Samsung Science and Technology Foundation under Project Number SSTF-BA1402-10. The quantum calculations were performed using the supercomputing resources of the Korea Institute of Science and Technology Information (KISTI). The work at Kyoto University was financially supported by the Global Research Laboratory (GRL, 2013K1A1A2A0205183) Program funded by the Ministry of Education, Science and Technology of Korea (MEST). The work at Pusan National University was supported by the National Research Foundation of Korea (NRF) grant funded by the MEST (NRF-2014R1A2A2A01002456).

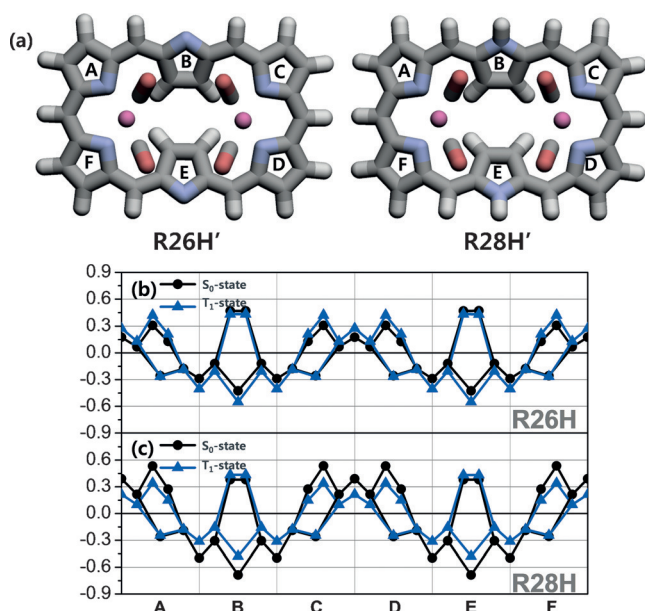


**Figure 3.** a) Molecular structures of non-substituted bis(rhodium) hexaphyrins (**R26H'** and **R28H'**) showing the positions for the mean-plane deviations. C gray, N blue, Rh purple, O pink. b) Diagram for the mean-plane deviations of **R26H** c) Diagram for the mean-plane deviations of **R28H**.

**Keywords:** aromaticity reversal · Baird's rule · hexaphyrins · time-resolved IR spectroscopy

**How to cite:** *Angew. Chem. Int. Ed.* **2016**, 55, 11930–11934  
*Angew. Chem.* **2016**, 128, 12109–12113

- [1] V. I. Minkin, M. N. Glukhovtsev, B. Y. Simkin, *Aromaticity and Antiaromaticity: Electronic and Structural Aspects*, Wiley, New York, **1994**.
- [2] E. Hückel, *Z. Phys.* **1931**, 70, 204–286.
- [3] N. C. Baird, *J. Am. Chem. Soc.* **1972**, 94, 4941–4948.
- [4] H. Ottosson, *Nat. Chem.* **2012**, 4, 969–971.
- [5] M. Rosenberg, C. Dahlstrand, K. Kilså, H. Ottosson, *Chem. Rev.* **2014**, 114, 5379–5425.
- [6] J.-i. Aihara, *Bull. Chem. Soc. Jpn.* **1978**, 51, 1788–1792.
- [7] P. Ilić, B. Sinković, N. Trinajstić, *Isr. J. Chem.* **1980**, 20, 258–269.
- [8] F. Fratev, V. Monev, R. Janoschek, *Tetrahedron* **1982**, 38, 2929–2932.
- [9] V. Gogonea, P. v. R. Schleyer, P. R. Schreiner, *Angew. Chem. Int. Ed.* **1998**, 37, 1945–1948; *Angew. Chem.* **1998**, 110, 2045–2049.
- [10] S. Zilberg, Y. Haas, *J. Phys. Chem. A* **1998**, 102, 10843–10850.
- [11] T. M. Krygowski, M. K. Cyrański, *Tetrahedron* **1999**, 55, 11143–11148.
- [12] P. W. Fowler, E. Steiner, L. W. Jennesken, *Chem. Phys. Lett.* **2003**, 371, 719–723.
- [13] S. Villaume, H. A. Fogarty, H. Ottosson, *ChemPhysChem* **2008**, 9, 257–264.
- [14] P. B. Karadakov, *J. Phys. Chem. A* **2008**, 112, 7303–7309.
- [15] P. B. Karadakov, *J. Phys. Chem. A* **2008**, 112, 12707–12713.
- [16] F. Feixas, J. Vandenbussche, P. Bultinck, E. Matito, M. Solà, *Phys. Chem. Chem. Phys.* **2011**, 13, 20690–20703.
- [17] R. Papadakis, H. Ottosson, *Chem. Soc. Rev.* **2015**, 44, 6472–6493.
- [18] H. Möllerstedt, M. C. Piqueras, R. Crespo, H. Ottosson, *J. Am. Chem. Soc.* **2004**, 126, 13938–13939.
- [19] H. Ottosson, et al., *Chem. Eur. J.* **2007**, 13, 6998–7005.
- [20] M. Rosenberg, H. Ottosson, K. Kilså, *Phys. Chem. Chem. Phys.* **2011**, 13, 12912–12919.
- [21] K. Jorner, et al., *Chem. Eur. J.* **2014**, 20, 9295–9303.
- [22] J. Zhu, K. An, P. v. R. Schleyer, *Org. Lett.* **2013**, 15, 2442–2445.
- [23] K. An, J. Zhu, *Eur. J. Org. Chem.* **2014**, 2764–2769.
- [24] I. McAuley, E. Krogh, P. Wan, *J. Am. Chem. Soc.* **1988**, 110, 600–602.
- [25] D. Shukla, P. Wan, *J. Am. Chem. Soc.* **1993**, 115, 2990–2991.
- [26] H. J. Wörner, F. Merkt, *Angew. Chem. Int. Ed.* **2006**, 45, 293–296; *Angew. Chem.* **2006**, 118, 299–302.
- [27] Y. M. Sung, et al., *Nat. Chem.* **2015**, 7, 418–422.
- [28] Y. M. Sung, et al., *J. Am. Chem. Soc.* **2015**, 137, 11856–11859.
- [29] H. Rath, et al., *Chem. Commun.* **2009**, 3762–3764.
- [30] D. A. Skoog, F. J. Holler, S. R. Crouch, *Principles of Instrumental Analysis*, 6th ed., Thomson, Brooks/Cole, Belmont, **2007**.
- [31] S. Kim, M. Lim, *J. Am. Chem. Soc.* **2005**, 127, 8908–8909.
- [32] S. Kim, J. Park, T. Lee, M. Lim, *J. Phys. Chem. B* **2012**, 116, 6346–6355.
- [33] M. Stępień, N. Sprutta, L. Latos-Grażyński, *Angew. Chem. Int. Ed.* **2011**, 50, 4288–4340; *Angew. Chem.* **2011**, 123, 4376–4430.
- [34] S. Saito, A. Osuka, *Angew. Chem. Int. Ed.* **2011**, 50, 4342–4373; *Angew. Chem.* **2011**, 123, 4432–4464.
- [35] J.-Y. Shin, et al., *Chem. Soc. Rev.* **2010**, 39, 2751–2767.
- [36] S. Cho, et al., *J. Phys. Chem. Lett.* **2010**, 1, 895–900.
- [37] W. Jentzen, J.-G. Ma, J. A. Shelnutt, *Biophys. J.* **1998**, 74, 753–763.
- [38] M. Suzuki, A. Osuka, *Chem. Commun.* **2005**, 3685–3687.
- [39] W.-Y. Cha, et al., *Chem. Eur. J.* **2012**, 18, 15838–15844.

Received: April 14, 2016

Published online: August 11, 2016